

DEFENCE S&T TECHNICAL BULLETIN

VOL. 14 NUM. 1 YEAR 2021 ISSN 1985-6571

CONTENTS

- Application of Design of Experiment Technique for Optimisation of Laboratory Scale Soda Lime Processing 1 - 11
Mahdi Che Isa, Nik Hassanuddin Nik Yusoff, Mohd Subhi Din Yati, Mohd Moesli Muhammad, Hasril Nain & Azmahani Sulaiman
- Decontamination of Chemical Warfare Agent by Nanocomposite Adsorbent: A GC-MS Study 12 - 19
Faris Rudi, Norliza Hussein, Siti Noriza Kamel, Hidayah Aziz & Azlan Nor Rashed
- Comparison of Physical Activity Ratio of Specific Physical Activities Performed by Military Personnel in Malaysia Using a Selection of Prediction Equations for Basal Metabolic Rate 20 - 25
Brinnell Caszo, Hanapi Johari & Justin Gnanou
- Characterisation of Mechanical-Electrical Properties of Graphene Nanoplatelets Filled Epoxy as Conductive Ink 26 - 42
Maizura Mokhlis, Mohd Azli Salim, Nor Azmmi Masripan, Adzni Md. Saad, Feng Dai, Azmi Naroh & Mohd Nizam Sudin
- Measurement of Optimal Stretchability Graphene Conductive Ink Pattern by Numerical Analysis 43 - 54
Ameeruz Kamal Ab Wahid, Mohd Azli Salim, Murni Ali, Nor Azmmi Masripan, Feng Dai & Adzni Md Saad
- Drag Reduction of Separate Lift Thrust (SLT) Vertical Take-Off and Land (VTOL) Components 55 - 69
Zulhilmy Sahwee, Muhd Hariz Asri, Nadhiya Liyana Mohd Kamal, Norhakimah Norhashim, Shahrul Ahmad Shah & Wan Nursheila Wan Jusoh
- Development of Video Data Post-Processing Technique: Generating Consumer Drone Full Motion Video (FMV) Data for Intelligence, Surveillance and Reconnaissance (ISR) 70 - 81
Muhammad Akmal Asraf Mohamad Sharom, Mohd Fazuwan Ahmad Fauzi, Abd Razak Sipit & Mohamad Zulkhaibri Mat Azmi
- Assessment and Mitigation of Monsoon Floods via Satellite Imagery Data Extraction and Drone Full Motion Video (FMV) 82 - 90
Muhammad Akmal Asraf Mohamad Sharom, Mohd Fazuwan Ahmad Fauzi, Mohamad Zulkhaibri Mat Azmi, Syariman Samsudin, Mohd Hakimi Abdul Rahman, Mohammad Azizi Fadzil & Sabrina Shahri
- Solar Irradiance Forecasting Using Global Positioning System (GPS) Derived Total Electron Content (TEC) 91 - 100
Angelin Anthony & Yih Hwa Ho



Ministry of Defence
Malaysia

SCIENCE & TECHNOLOGY RESEARCH
INSTITUTE FOR DEFENCE (STRIDE)

CHARACTERISATION OF MECHANICAL-ELECTRICAL PROPERTIES OF GRAPHENE NANOPATELETS FILLED EPOXY AS CONDUCTIVE INK

Maizura Mokhlis¹, Mohd Azli Salim^{1,2,*}, Nor Azmmi Masripan¹, Adzni Md. Saad¹, Feng Dai³, Azmi Naroh⁴ & Mohd Nizam Sudin¹

¹Fakulti Kejuruteraan Mekanikal, Universiti Teknikal Malaysia Melaka (UTeM), Malaysia

²Advanced Manufacturing Centre, Universiti Teknikal Malaysia Melaka (UTeM), Malaysia

³China Railway Eryuan Engineering Group Co., China

⁴Department of Mechanical Engineering, Politeknik Ungku Omar, Malaysia

*Email: azli@utem.edu.my

ABSTRACT

With the accelerating pace of development in printed electronics, the fabrication and application of conductive ink have been brought into sharp focus in recent years. The discovery of graphene also unfolded a vigorous campaign on its application. The purpose of this study was to determine the effect of graphene ink when the heat was applied to obtain the optimised formula and prepare graphene conductive ink with good conductivity. In this paper, graphene conductive ink was prepared using a simple method involving mixing, printing, and curing processes to produce conductive ink according to the formulation. Different compositions of a mixture that contained filler, binder, and hardener were put inside a vacuum to remove bubbles and the ink was cured at 150°C for 30 minutes. This research also studied the effect of the temperature on electrical and mechanical properties, and surface roughness of the hybrid conductive ink using a varying amount of filler for graphene nanoplatelets (GNP) inks. The electrical and mechanical properties were assessed using a four-point probe complying with the ASTM F390 and a Dynamic Ultra Microhardness complying with the ASTM E2546-15. The experimental results demonstrated an improvement in electrical conductivity. GNP showed resistivity around 0.0456 Mohm/sq. The correlation between the material hardness with different percentages of filler loading for GNP ink with and without thermal effect conditions was presented. Both of the two GNP ink conditions exhibited similar graph trends, where the hardness was found to increase as the filler loading in the ink was increased.

Keywords: *Graphene ink; sheet resistivity; surface roughness; cross-section; hardness.*

1. INTRODUCTION

In the last few years, the development of technologies for conductive ink grew significantly. Conductive ink has been pushed forward by the progress of printed and flexible electronics (Rosa *et al.*, 2015). Printed electronics are involved in the development of electrical and electronic system printing techniques on different types of substrates. It is an emerging technology, which grows rapidly due to its wide application in radio frequency identification (RFID) (Huang *et al.*, 2015; Leng *et al.*, 2016), chemical sensors (Singh *et al.*, 2017; Tortorich *et al.*, 2018) and wearable electronics (Van Den Brand *et al.*, 2015; Gao *et al.*, 2017). There is an ever-increasing need to develop and produce electronic devices with new characteristics, which have low manufacturing costs, long-endurance time, environmentally sustainable production methods, recycling ability, lower energy consumption, and higher efficiency.

To meet all the requirements, a new manufacturing technique must be developed, and new advanced materials must be taken into use. One of the promising manufacturing techniques for electronic production is printing. Printing is an additive method, which can be used to prepare conductive pattern

directly on flat or even with differently shaped and curved surfaces. Different printing techniques like screen printing, gravure printing, and flexographic printing have been used to fabricate electronic circuits. These printing techniques offer a way to manufacture electronic circuits onto several materials such as paper, plastic, and fabric and make the integration process possible.

Conductive ink consists of conductive materials, polymer matrix, solvents, and additives. Generally, the conductive materials used involve metal nanoparticles (Vasiljevic *et al.*, 2013), carbon nanotubes (Lau *et al.*, 2013), and graphene (Eawwiboonthanakit *et al.*, 2017). Nanomaterials, which possess high carrier mobility, optical transparency, mechanical robustness and flexibility, lightweight and environmental stability have been in immense demand. Graphene is one of the nanomaterials that fulfill all these requirements, along with other inherently unique properties and convenience to fabricate into different morphological nanostructure, from atomically thin single layers to nanoribbon (Atif *et al.*, 2016; Mokhlis *et al.*, 2020). So far, three kinds of graphene-related conductive ink have been fabricated, which are pristine graphene (PG) ink (Wajid *et al.*, 2013), graphene oxide (GO) ink (Abdullah & Ansari, 2015), and reduced graphene oxide (RGO) ink (Huang *et al.*, 2011). Each kind of ink has its pros and cons.

This research is focusing on graphene nanoplatelets (GNP). GNP consist of a small stack of graphene sheet with a platelet shape as shown in Figure 1 and are highly used as filler in the study of polymer composites. The geometrical structure of GNP, with the particle size of nanoscale thickness and micron-scale lateral surface area allows a high surface contact area. By embedding the polymer matrix at low filler loading, it improves the properties of the polymer matrix without sacrificing any intrinsic properties. To form conductive ink, epoxy resin is the most compatible polymer binder due to its viscosity behaviors. It is also the most extensively used thermoset polymer in the composite industry. It is frequently used in demanding applications due to excellent chemical and corrosion resistance, outstanding adhesion properties, low shrinkage, and low price (Wei *et al.*, 2015). As for hardener, it is a solvent that is added to the ink mixture to harden and produce strong and more durable ink as well as a curing agent for epoxy.

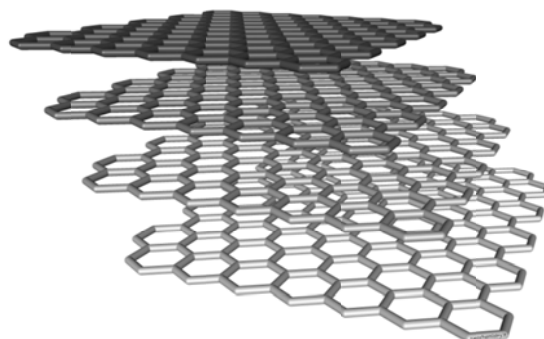


Figure 1: Crystal structure of GNP (Kucinski *et al.*, 2013).

In general, conductive ink is composed of a conductive phase with ink binder and additives in a solvent. The conductive phase plays the role of conducting current and ink binder dissolves in a solvent to connect the conductive phase, while additives are used to adjust the printability of conductive ink. The major issue to be resolved in the formulation of conductive ink should not only focusing on the synthesis of raw material but also the ink formulation to improve the stability and dispersion of the ink. The ink originally comes in liquid form and will be drawn on a substrate and cured afterward. The ink draws on the substrates is usually cured with an oven. These processes use heat to evaporate binders and unwanted solvent in conductive ink polymers, which leave only the nanoparticles contents that are already been hardened and stick onto the substrate. Curing is the process to crosslink the polymer materials that can form a good composition with excellent properties.

One of the major challenges is to formulate suitable inks that can be printed using printing technologies in order to replace conventional technologies, which create a limitation in terms of an environmental issue (Faddoul *et al.*, 2012; Wu, 2017). Up to now, numerous kinds of conductive ink with different fillers such as silver, copper, and carbon-based material have been developed for the formation of conductive ink. Typically, silver and copper inks have been globally commercialised and used in electronic industries due to their excellent electrical conductivity performance. However, the problems with silver ink are the high cost, low content, and electromigration behaviour that limit their widespread industrial application.

Other than that, copper is an attractive alternative material to silver due to its comparable bulk conductivity. However, copper is easily oxidised, and the presence of copper oxide increases sintering temperature and reduces conductivity (Lee *et al.*, 2008; Nie *et al.*, 2012; Yang *et al.*, 2016). Thus, there is still a need to develop new types of conductive ink to solve the above-mentioned problem. Therefore, carbon-based material is utilised in this study as the filler material, which is graphene nanoplatelets (GNP) with different filler percentages to investigate the role of those properties in the enhancement of functionality and reliability of the conductive ink (Ismail *et al.*, 2020).

2. METHODOLOGY

2.1 Materials

Graphene nanoplatelets with a surface area of 500 m²/g were used as the main filler in this study. Binder system bisphenol, an epoxy resin BE-188 (BPA) was used as a binder to bind the particles together, and ACR Hardener H-2310 polyamide amine to harden the mixture.

2.2 Ink Preparation

The fabrication of graphene conductive ink involves formulating the ink composition, preparing the ink sample, printing the ink on the compatible substrate, and curing at the temperature of 150°C for 30 minutes. For the first condition, namely mixing without thermal effect, the stirring process took 15 minutes continuously at room temperature (25°C) by using a glass rod. For the second condition, namely mixing with thermal effect, the stirring process took 15 minutes continuously with the addition of heat at 70°C. The preheated mixture was taken into the vacuum to remove the bubbles. The conductive ink was prepared with six (6) different percentages of filler loading: 10, 15, 20, 25, 30, and 35 wt.% with the hardener in the ratio of 100:30. The composition of the filler loading is tabulated in Table 1.

Table 1: The composition of graphene ink.

Sample	Filler		Binder		Hardener (g)	Total (g)
	(%)	(g)	(%)	(g)		
1	10	0.2	90%	1.8	0.54	2
2	15	0.3	85%	1.7	0.51	2
3	20	0.4	80%	1.6	0.48	2
4	25	0.5	75%	1.5	0.45	2
5	30	0.6	70%	1.4	0.42	2
6	35	0.7	65%	1.3	0.39	2

The ink was prepared by manual mixing that involved a stirring process by using a glass rod. Stirring plays an important role in ensuring the uniform distribution of epoxy in the mixture and it can break up the agglomerates of GNP and epoxy resin to produce high GNP/epoxy dispersion. The experiment started with the deposition of the inked track onto a glass substrate using the doctor blade technique. A doctor blade method was used to deposit the ink, in which a metal stencil and low tack tape were applied on a polymer substrate. The stencil was placed on the tape polymer substrate and a knife was

used to cut the tape accordingly to leave a negative shape of the track image. The stencil was then removed, and the negative track of the tape was then flooded with ink and a scraper was used to draw across the surface of the tape. Once it had properly flooded and scraped with the excess ink removed, the tape was peeled off and left a positive image of ink (Nash *et al.*, 2015).

The ink track samples were then transferred into the oven to undergo a curing process. During the curing process, it produces a highly-cross-linked microstructure that provides high modulus and strength, good resistance to creep, and good performance at elevated temperatures. Then, the cured sample was cooled down slowly to room temperature inside the oven. The curing process had been set up at 150°C for 30 min with an increment of the filler loading. The result turned out to be as expected, in which the higher the filler loading resulting in better performance of ink track. The resistance of the inked track increased as the filler loading increased, which gave better conductivity. Optimised graphene conductive ink was printed on a glass slide with a size of 7.5 cm x 0.3 cm and cured to test the resistance value using uniformity and continuity tests. For the uniformity test, the printed graphene ink was divided into six-point as shown in Figure 4. The resistance value was tested for each centimetre along the length direction. Then the test length was increased per centimetre for the continuity test. All the data for each of the graphene printed ink samples were collected for three repetitions and the average values and standard deviations (error bar) were obtained.

2.3 Sample Characterisation

This study is focusing on examining the morphological, electrical, and mechanical properties of the graphene nanoplatelets (GNP) reinforced epoxy composite. In order to evaluate these properties, the samples were prepared specifically according to each relevant testing standard. Nine marks were constructed at each ink layer in one sample to specify upper, middle, and lower positions as shown in Figure 2. The average values from these marks became the results and the details were discussed.

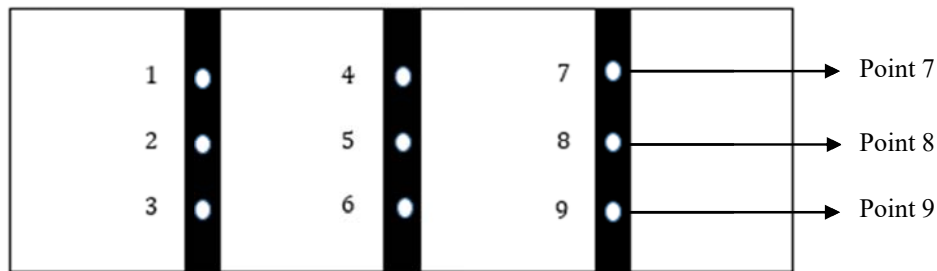


Figure 2: Schematic diagram of printed ink on a glass slide.

2.3.1 Morphology Properties

Scanning electron microscopy (SEM) was used to investigate and evaluate the cross-section of the printed sample. Furthermore, the auto fine machine coating was used to coat the printed sample in order to avoid charge accumulation. SEM employs electron beams to get information from a sample at the nanoscale. The main signals that are detected are the backscattered (BSE) and secondary electron (SE), which generate a grayscale image of the sample at very high magnification. However, there are many other signals which can be the products of electron-matter interaction, and these can provide additional information about the sample such as energy dispersive x-ray (EDX). The data that is generated by EDX analysis consists of spectra with peaks corresponding to all the different elements that are present in the sample. This study investigated the distribution between filler reinforced binder at different filler loadings. The distribution state of nanofillers is crucial to the nanocomposites. Chandrasekaran *et al.* (2014) reported that the homogenous dispersion of nanofillers was an important factor affecting the mechanical properties of the composites (Chandrasekaran, 2014).

2.3.2 Electrical Properties

The electrical properties of cured samples were measured to determine their functions. In this study, the sheet resistance of the conductive ink was determined using JANDEL In-Line Four Point Probes with a 1 mm distance between each probe by referring to ASTM F390 as shown in Figure 3. To measure the resistance of the cured ink, the probe was held in firm contact with the inked track. The four-point probe works by forcing a constant current along with two outer probes and the voltage is read out from the two inner probes. Each data point was obtained as an average of twelve different measurements on the sample.

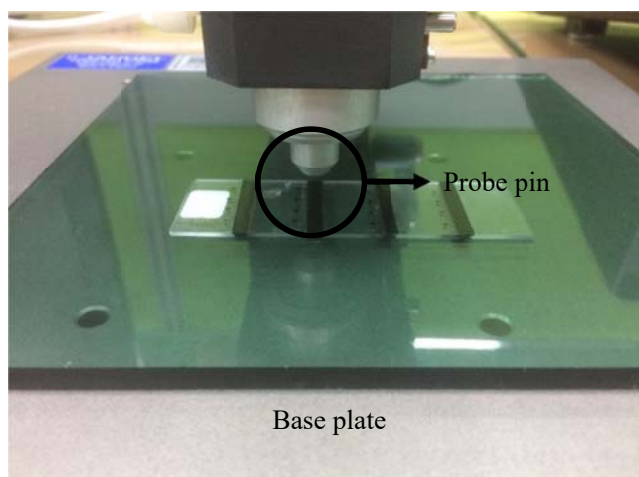


Figure 3: Four-point probe sample preparation.

2.3.3 Mechanical Properties

Nanoindentation analysis was carried out using Dynamic Ultra Micro Hardness testing using a three-sided pyramidal (Berkovich) diamond tip. The nanoindenter test was conducted to describe the elastic behavior of the printed ink. The test method used was the continuous stiffness method (CSM), which is able to plot the curve of hardness and modulus by continuously varying indentation depth. The nine indentations had been made for each sample. Each sample was measured at nine different positions. During each test run, a personal computer collected and stored data for the load and displacement as the indenter was driven into the sample. Then, the raw data was used to construct the load-displacement graph.

2.3.4 Surface Roughness

A 3D non-contact profilometer was used to measure the surface profile to quantify its roughness. It greatly depended on the surface geometry of the printed pattern such as thickness and roughness. The leading method of this type of technique is light. Emitted light from the instrument is reflected and read to measure without touching the sample. The thickness was measured using I-solution lite software connected to an optical microscope. The thickness values were the average values from nine different measurement points on the ink tracks. Minimum, maximum, and standard deviation were also calculated by the software. The surface roughness values of R_a and R_z of the substrate were measured using a profilometer.

3. RESULTS & DISCUSSION

All the collected data and results obtained from the experiment and tests were analysed and recorded. The resistivity, stability, and microstructure of ink were discussed to find out the best ink formulation based on the recorded data. The result turned out to be as expected in which the higher the filler loading resulting in better performance of the ink track. The resistance of the inked track increased as the filler loading increased and it gave better conductivity.

3.1 Morphological Properties

The enhancement of the properties is strongly correlated with nanocomposite microstructure. Effective characterisation of morphology is important to establish a structure-property relationship for these materials. Scanning electron microscopy (SEM) had been used to evaluate the dispersion of GNP as well as to examine the surface for filler pull out, which could give insight into the strength of interfacial adhesion. There were six samples as shown in Figures 4 (a) and (b) and Figures 5 (a) and (b). It shows that 10 wt.% and 15 wt.% of GNP inks with and without thermal effect have brighter images and uneven distribution on the cross-sectional area. The micrograph also shows bad dispersion with many small and black clusters of GNP inks.

Comparatively, the dispersion of low filler loading of 10 wt.% and 15 wt.% between the GNP inks with and without thermal effect does not change significantly, but the aggregate size indeed becomes smaller as shown in Figures 4 (a) and (b) and Figures 5 (a) and (b). Hence, they do not show the existence of resistivity as they contain a low percentage of filler loading (Chatterjee *et al.*, 2012). Starting from 20 wt.% of filler loading as shown in Figures 4 (c) and Figure 5 (c), the cross-sectional images have shown smooth, homogeneous, and continuous cross-sectional areas on the GNP inks. In the same figures, they illustrate that the GNP inks distribute uniformly on the substrate and even further, GNP ink can be dispersed and stabilised well in the conductive ink.

From Figures 4 (e) and (f) and Figures 5 (e) and (f), they show a smooth surface, which reveals the nature of weak resistance to crack initiation and propagation. On the other hand, composite containing a high percentage of filler loading exhibits relatively rough with some river-like structure. Comparatively, the composite with the highly dispersed GNP inks exhibits a rougher surface and numerous tortuous and fine river-like structures with hackles and ribbons. This result was similar to one of the studies that had been reported (Tang *et al.*, 2013). Therefore, Figures 4 and 5 show the cross-sectional area of GNP ink without thermal effect and GNP ink with thermal effect.

In EDX, the y-axis depicts the number of counts and the x-axis illustrates the energy of x-rays as shown in Figures 6 and 7. The position of the peaks leads to the identification of the element concentration in the sample. Samples of 10 wt.% of graphene ink with and without thermal effect have an atomic weight of 74.88 % and 69.00 %, while for the samples of 35 wt.% are 84.00 % and 100.00% respectively. The higher the atomic weight of graphene, the lower the resistance of conductive ink track because the lesser amount of carbon particle that obstructs the movement of electron between graphene particles.

Electrical conductivity is the measurement regarding the ability of a material to transfer or conduct an electric current. Lower resistance means that the material will conduct electricity more easily than a material with high resistance.

$$\sigma = \frac{1}{\rho} \quad (2)$$

where σ is conductivity.

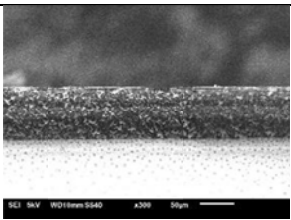
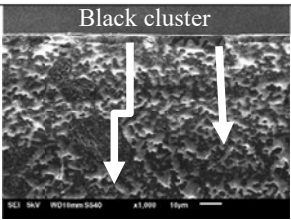
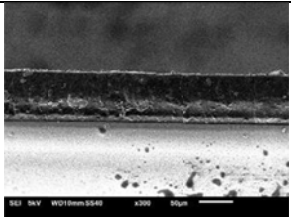
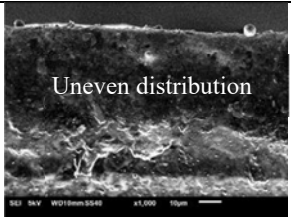
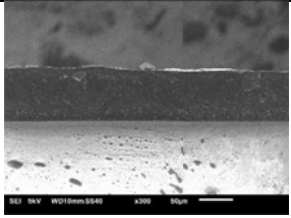
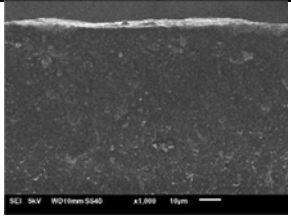
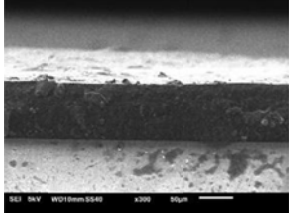
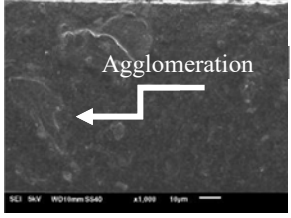
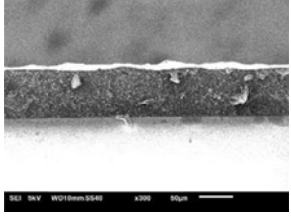
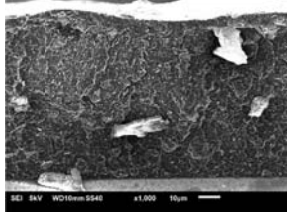
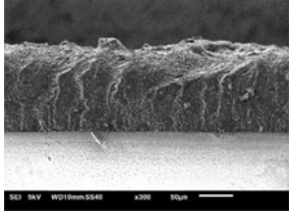
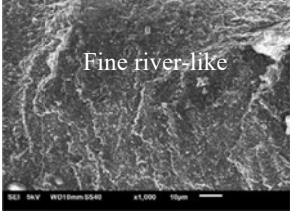
Filler loading	GNP ink without thermal effect	
	x300	x1000
(a) 10 wt.%		
(b) 15 wt.%		
(c) 20 wt.%		
(d) 25 wt.%		
(e) 30 wt.%		
(f) 35 wt.%		

Figure 4: The cross-sectional areas of GNP ink without thermal effect.

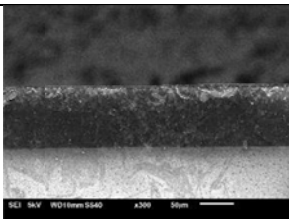
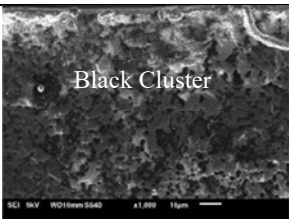
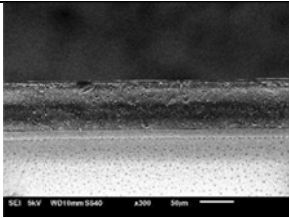
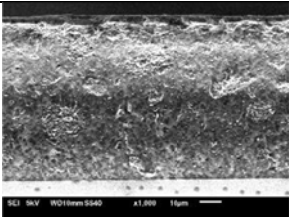
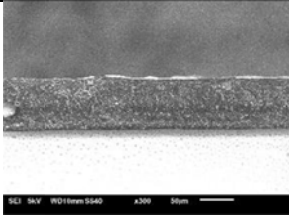
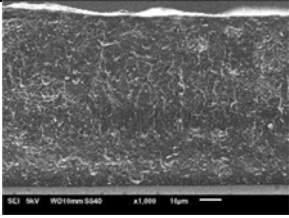
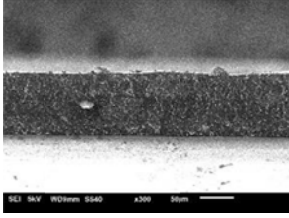
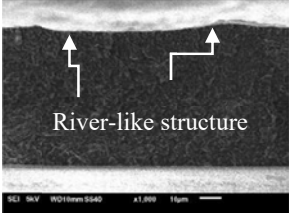
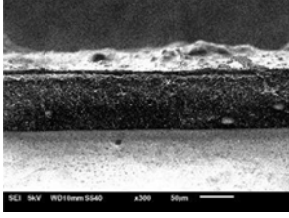
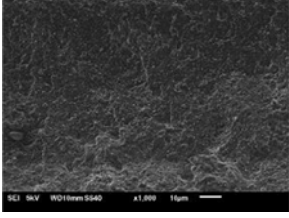
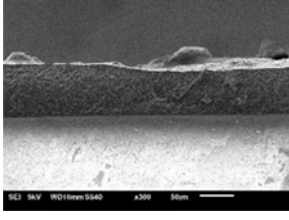
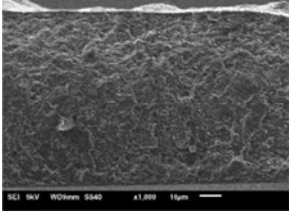
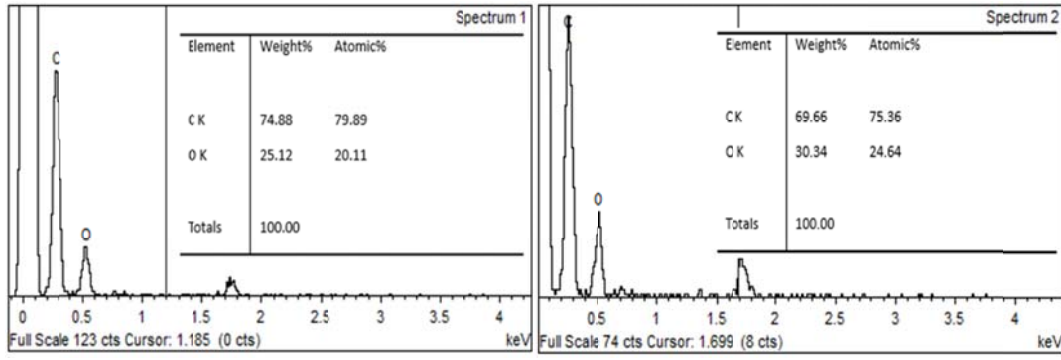
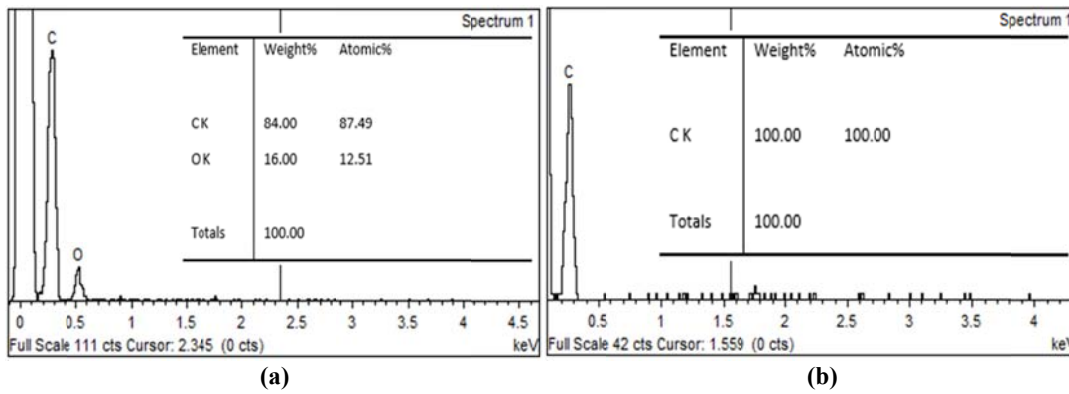
Filler loading	GNP ink with thermal effect	
	x300	x1000
(a) 10 wt.%		
(b) 15 wt.%		
(c) 20 wt.%		
(d) 25 wt.%		
(e) 30 wt.%		
(f) 35 wt.%		

Figure 5: The cross-sectional areas of GNP ink with thermal effect.



**Figure 6: EDX analysis showing the content of sample 10 wt.%.
(a) GNP ink without thermal effect (b) GNP ink with thermal effect.**



**Figure 7: EDX analysis showing the content of sample 35 wt.%.
(a) GNP ink without thermal effect (b) GNP ink with thermal effect.**

3.2 Electrical Properties

For the printed samples of both GNP ink with and without thermal effect, the resistance is opposing the flow of electrons through the material in response to an applied voltage. Conductors have very small resistances and allow electrons to flow easily if a voltage is applied. Insulators have large resistance and do not allow electrons to flow easily. In order to prove how easily the sample conduct electricity, a device called a four-point probe was used to measure the resistance. When the probe was connected to the printed samples, the voltage was supplied and then the current through the ink was measured at the given voltage. The relationship between resistance and resistivity is important to be understood when describing the printable conductor. Resistance is a measurement for an object to resist or oppose an electric current that flows through it. The electrically resistive nature of the material is an intensive property, which is known as resistivity. The resistance depends on the physical shape and pattern, but the resistivity depends on the nature of the material. The relationship between resistance and resistivity is shown below:

$$\rho = \frac{A}{L} R \quad (1)$$

where ρ is volume resistivity, A is cross-sectional area, L is length, and R is resistance.

Table 2 shows the average value of sheet resistance and the standard deviation for six (6) percentages of filler loading. Each sample consists of six points to measure the uniformity of the printed GNP ink. Therefore, there is no standard benchmark in determining the standard deviation, but the lowest value indicates the best standard deviation. It presents how tightly the data is gathered around the mean or average or how far the data is spread out from the mean or average. The table below shows that 20 wt.% of GNP ink without thermal effect has a very large standard deviation as compared to 20 wt.% of GNP ink with thermal effect.

Table 2: The sheet resistance value of GNP ink.

	Filler loading	10wt.%	15wt.%	20wt.%	25wt.%	30wt.%	35wt.%
Sheet resistance (MΩ/sq)	GNP without thermal effect	0	0	308.88	42.324	3.3519	0.0456
	Std	0	0	15.444	2.1162	0.1675	0.00228
	GNP ink with thermal effect	0	0	11.909	2.2913	0.1616	0.1431
	Std	0	0	0.5954	0.1145	0.00808	0.00715

Figure 8 shows the sheet resistivity against the percentage of filler loading for both graphene inks in two conditions, with and without thermal effect. In general, regardless of adding the temperature to the mixture, the sheet resistivity of the ink decreases with an increase in the filler loading from 10 wt.% to 35 wt.%. In other words, better electrical conductivity is achieved by increasing the filler loading. Such observation is supported by percolation theory, which states that filler content in conductive polymer composite reaches its critical volume that varies, based on the filler's physical properties such as shape and size. Upon reaching the critical volume, the filler forms a three-dimensional conductive network within the polymer matrix and resulting in a dramatic decrease in the sheet resistance (Saad *et al.*, 2020).

From all the prepared samples, the results reveal that only four samples have the existence of resistivity, which are from 20 wt.% to 35 wt.%. For 10 wt.% and 15 wt.%, there is no existence of resistivity due to the small amount of filler loading. A small amount of filler loading leads to an agglomeration effect. No electrical conductivity is produced due to the agglomeration effect. Therefore, there are no resistivity values can be obtained. The different range of resistivity at different filler loadings on the samples is shown in Figure 8. From the graph, 35 wt.% of the ink mixture shows lower resistivity. It is proven that the higher the percentage of filler loading, the lower the resistivity.

There is a major difference between the values of resistivity of 20 wt.% to 25 wt.% for GNP ink without thermal effect. It is because of the possibility that the ink is not well-distributed all over the gap between the scotch tape on the glass slide when the blade is moved across the gap due to the speed or the viscosity of the ink. When the speed of the blade increases, the ink may lose and not covering all the gap area. As for the viscosity of the ink, it increases with higher filler content. Ink with high viscosity is hard to print in compliance with the texture of the ink. Thus, it causes the inconsistent thickness of printed inks on the glass side. Some regions may have different thickness, which leads to different spreads of conducting material.

There is a significant difference in values before and after 15 wt.% of filler loading, which are 327.95 MΩ/sq for ink without thermal effect and 16.54 MΩ/sq for ink with thermal effect. However, when the loading reaches approximately 30 wt.%, it can be clearly seen that the sheet resistance has reached a plateau. This trend suggests that the conductive ink has been transformed from bulk insulator to bulk electrical conductor by the percolated network. In addition, during this state, the electrical performance of the ink is determined by intrinsic filler material properties (Lu, 2012). Furthermore, the higher content of filler loading is needed to make good physical contact with other fillers to building up the conductive network.

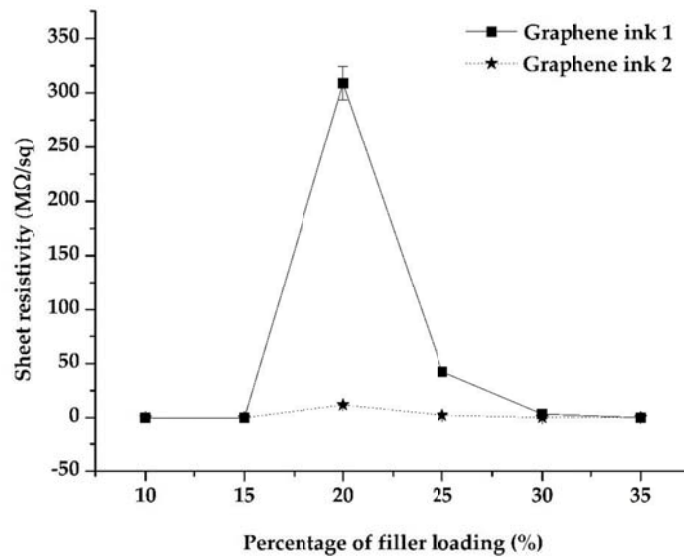


Figure 8: The graph of sheet resistance against filler loading.

3.3 Mechanical Properties

Graphene has excellent mechanical properties, particularly high Young's modulus. These exceptional properties make graphene an ideal candidate as a filler for nanocomposites materials. This Graphene ink is aimed to be exploited due to remarkable mechanical enhancement effect with the possibilities to introduce further functionalities such as electrical conductivity. For this study, nanoindentation analysis was carried out using the method described by Deng in 2013. Two frequently measured mechanical properties are Young's modulus and hardness. As the indenter is driven into the material, both elastic and plastic deformations cause the formation of hardness. After the indenter is withdrawn, only the elastic portion of the displacement is recovered, thus this recovery enables one to determine the elastic properties of a material. Therefore, the first step of measurement was preparing the sample by mounting it on a sample disk (Oliver *et al.*, 2004). The load-displacement graph shows the typical load-indentation depth curve obtained by nanoindentation for screen printed graphene ink. There is a possibility that the curve shows a similar trend, but the indentation and elastic behaviour are not the same.

Table 3 shows the maximum force, maximum depth, hardness, and elastic modulus for GNP ink without thermal effect (graphene ink 1) and GNP with thermal effect (graphene ink 2). The maximum penetration depth of all the graphene ink samples starting from 10 wt.% to 35 wt.% is at the same curing temperature. It clearly shows that the higher the percentage of filler loading causes a lower penetration depth. The lower the penetration depth indicates that the printed graphene ink is getting hardened.

As for Figure 9, it shows that when the filler increases, the hardness level of the printed graphene ink sample is also increasing accordingly. For GNP without thermal effect (graphene ink 1), the value increases in parallel with the increase of filler loading with 12.6 HV to 35.6 HV. While for GNP with thermal effect (graphene ink 2), the value of hardness also increases from 12.3 HV to 37.4 HV respectively. Similarly, this study is consistent with the result of Chatterjee in 2012, who reported an increase of approximately 0.266 GPa for the neat epoxy up to 0.290 GPa for 20 wt.% of GNP loading.

Table 3: The result from nanoindentation for GNP ink

Filler loading	Maximum force, Fmax (mN)		Maximum depth, hmax (μm)		Hardness (HV)		Elastic Modulus, Eit (GPa)	
	GNP ink without thermal effect	GNP ink with thermal effect	GNP ink without thermal effect	GNP ink with thermal effect	GNP ink without thermal effect	GNP ink with thermal effect	GNP ink without thermal effect	GNP ink with thermal effect
10wt.%	323.16	334.1	10.7	10.5	12.6	12.3	5.324	12.01
15wt.%	351.15	398.6	10.7	10.4	13.1	15.1	7.341	14.07
20wt.%	601.4	572.1	10.4	10.3	27.5	23.2	7.128	13.28
25wt.%	633.3	593.6	10.2	10.1	31.1	30.1	6.863	6.315
30wt.%	713.2	655.3	10.2	10.1	34.7	34.5	8.047	6.374
35wt.%	744.6	759.5	10.2	10.1	35.6	37.4	8.722	8.531

In short, the nanoindentation results show an improvement in hardness for GNP ink without thermal effect (graphene ink 1). Therefore, hardness value also has a similar tendency with sintering temperature. This increment is closely associated with grain growth at a higher temperature. More grain growth at higher temperature improves the mechanical properties. Moreover, based on the nanoindentation result, it confirms that the toughness of the ink increases when the heat is applied during the mixing method.

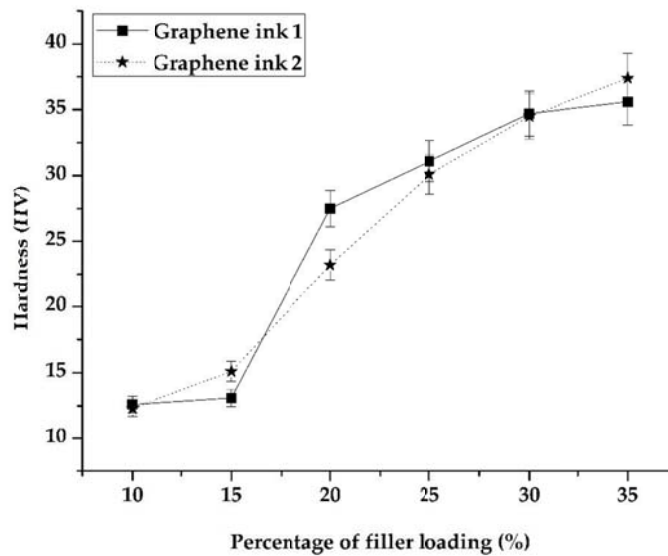


Figure 9: The graph of hardness against filler loading.

Moreover, Figure 10 indicates the result of Young's modulus of the samples of GNP ink without thermal effect (graphene ink 1) and GNP ink with thermal effect (graphene ink 2). As can be seen from Figure 10, it is expected that higher curing temperature leads to higher hardness and Young's modulus of the printed graphene ink. The elastic begins to degrade by increasing the curing temperature. This study assumes that, by adding the temperature, the properties of graphene ink will change from brittle to ductile. Therefore, graphene ink that cures at a higher temperature is likely to be stiffer. The result of this study was also compared with the findings of previous work. Previous

researchers had reported that the obtained values of Young's modulus were approximately 3.9 GPa to 4.2 GPa, which were lower than this study (Chatterjee *et al.*, 2012).

On the other hand, Figures 11 and 12 exhibit the maximum and minimum penetration depths achieve by the samples with lower and higher percentages of filler loading. The maximum penetration depth occurs at 10 wt.% with $h_{max}=10.7 \mu m$, meanwhile 35 wt.% acquires minimum penetration depth with $h_{max}=10.2 \mu m$ at the different peak load. As a result, the load indentation depth curve indicates that a lower percentage of filler loading yields a softer surface while for a higher percentage of filler loading yields a hardened surface. In summary, Figures 11 and 12 also gives a clear view that when the percentage of filler loading increases, the penetration of the indenter decreases steadily.

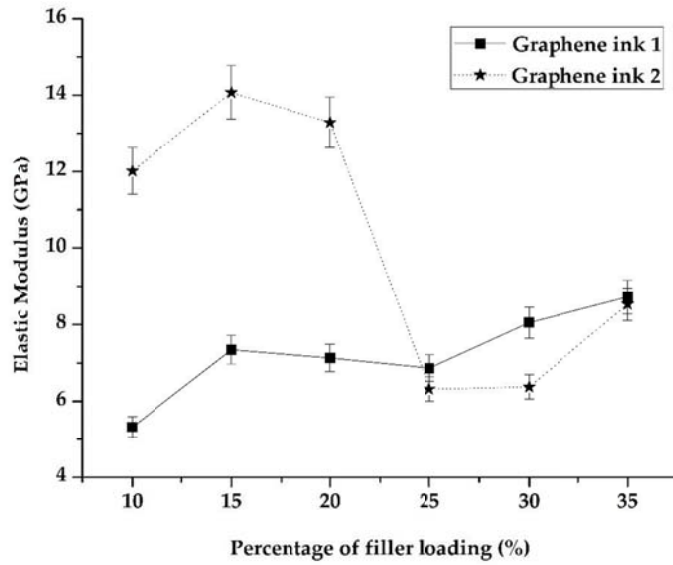


Figure 10: The graph of elastic modulus against filler loading

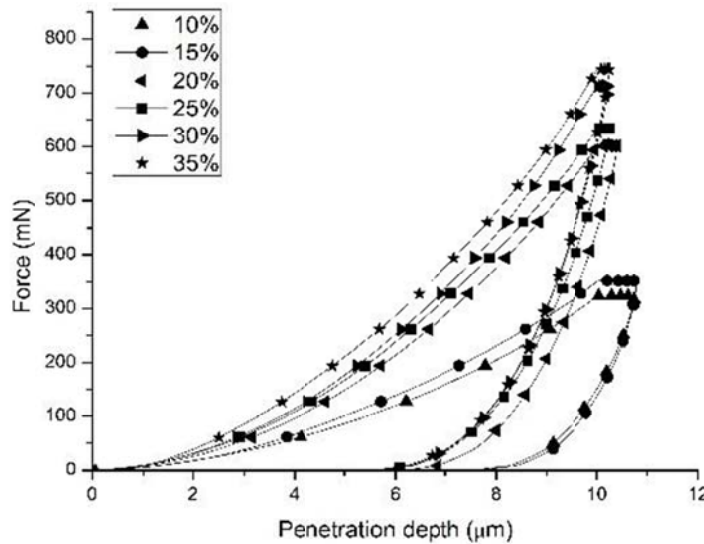


Figure 11: The load indentation curve for GNP ink without thermal effect (graphene ink 1)

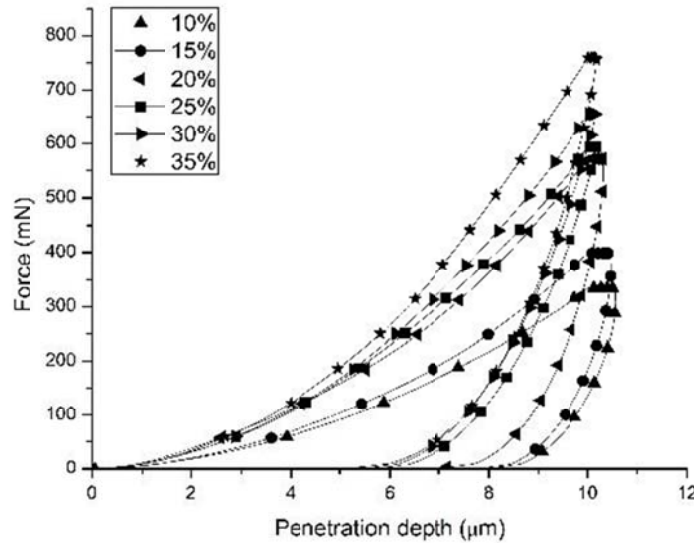


Figure 12: The load indentation curve for GNP ink with thermal effect (graphene ink 2)

3.4 Surface Roughness

In this study, the parameter used to assess the surface roughness was the average of roughness, Ra. Ra is the arithmetic average of surface height that is measured across a surface. In addition, it is a simple average of the height across the microscopic peaks and valleys. The result of surface roughness for six (6) filler loadings is shown in Table 4. Based on this table, the value of the surface roughness obtained is not consistent and uniform. The filler for 10 wt.% and 15 wt.% GNP ink without thermal effect have low surface roughness, which are 1.422 μm and 1.524 μm as compared to the surface roughness of GNP ink with thermal effect, which are 2.984 μm and 1.750 μm . The results for 10 wt.% to 20 wt.% of GNP ink without thermal effect also have stable consistency as compared to GNP ink with thermal effect. The lowest surface roughness, which means that it has the smoothest surface for GNP ink without thermal effect is 30 wt.% with 0.511 μm while for GNP ink with the thermal effect is 25 wt.% with 0.400 μm . The results for higher filler loading are slightly increasing for both conditions with 1.178 μm and 1.075 μm .

Figure 13 shows the graph of surface roughness against the filler loading. The surface roughness is barely the same for both conditions due to the thixotropic behavior of the ink and poor leveling. These lead to pore formation and very large height and depth between the two-line edge (Faddoul *et al.*, 2012). Surface roughness is one of many factors affecting electrical properties. According to Faddoul in 2012, it was estimated that surface roughness increases with the increase of filler content and viscosity. Furthermore, a study by Suherman in 2013 showed that the surface regularity, flatness, and microstructure are dependent on ink viscosity. Smooth surface allows continuous conductive line

formation without shorting risk, hence the hybrid shows a lower resistance compared to single fillers (Faddoul *et. al.*, 2012).

Table 4: The values of surface roughness

Filler loading	Surface roughness, (μm)			
	GNP ink without thermal effect	Average	GNP ink with thermal effect	Average
10 wt.%	0.981	1.422	3.421	2.984
	2.125		2.799	
	1.160		2.733	
15 wt.%	0.993	1.524	2.0145	1.750
	2.993		0.677	
	0.588		2.558	
20 wt.%	1.327	1.543	0.358	0.446
	1.650		0.487	
	1.654		0.494	
25 wt.%	1.306	1.051	0.315	0.400
	1.084		0.360	
	0.763		0.524	
30 wt.%	0.652	0.511	0.748	1.106
	0.523		1.361	
	0.359		1.209	
35 wt.%	0.863	1.178	1.671	1.075
	0.601		0.646	
	2.071		0.908	

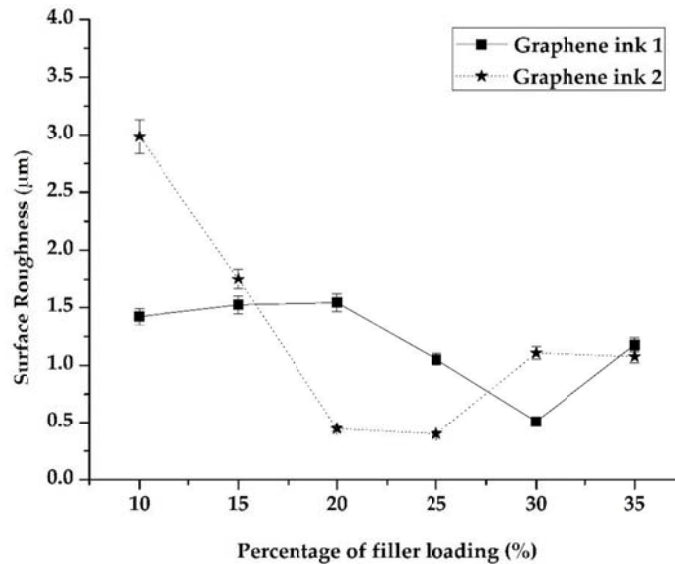


Figure 13: The graph of surface roughness against filler loading

4. CONCLUSION

Through the formulation of ink, all the processes including mixing, printing, and curing processes can be performed to fabricate the ink on the substrate. After the fabrication had been carried out, the behavior of conductive ink was investigated through electrical, mechanical, and morphological tests for GNP/epoxy conductive ink including the electrical and mechanical properties affected by

temperature, which was supplied during the mixing method, and the percentage of filler loading. However, the temperature of the mixing method did not give significant changes in mechanical properties and surface roughness. The percolation threshold for GNP was 30 wt.% at room temperature. Furthermore, the hardness increased with an increased percentage of elastic modulus. The trend contradicted for the hardness as the percentage of loading increased.

5. ACKNOWLEDGEMENT

Special thanks to the Advanced Manufacturing Centre (AMC) and Fakulti Kejuruteraan Mekanikal (FKM), Universiti Teknikal Malaysia Melaka (UTeM) for providing the laboratory facilities.

REFERENCES

- Abdullah, S.I. & Ansari, M.N.M. (2015). Mechanical properties of graphene oxide (GO)/epoxy composites. *HBRC J.*, **11**: 151-156.
- Atif, R., Shyha, I. & Inam, F. (2016). Mechanical, thermal, and electrical properties of graphene-epoxy nanocomposites—A review. *Polym.*, **8**: 281.
- Chandrasekaran, S. (2014). *Development of nano-particle modified polymer matrices for improved Improved fibre reinforced composite*. Doctoral dissertation, Universitätsbibliothek der Technischen Universität Hamburg-Harburg, Germany.
- Chatterjee, S., Nafezarefi, F., Tai, N.H., Schlagenhauf, L., Nüesch, F A. & Chu, B.T.T. (2012). Size and synergy effects of nanofiller hybrids including graphene nanoplatelets and carbon nanotubes in mechanical properties of epoxy composites. *Carbon*, **50**: 5380-5386.
- Deng, D., Jin, Y., Cheng, Y., Qi, T. & Xiao, F. (2013). Copper nanoparticles: aqueous phase synthesis and conductive films fabrication at low sintering temperature. *ACS Appl. Mater. Infer*, **5**: 3839-3846.
- Eawwiboonthanakit, N., Jaafar, M., Ahmad, Z., Ohtake, N. & Lila, B. (2017). Fabrication of PEDOT: PSS / graphene conductive ink printed on flexible substrate. *Solid State Phenom.* 264: 70-73.
- Faddoul, R., Reverdy-Bruas, N. & Blayo, A. (2012). Formulation and screen printing of water based conductive flake silver pastes onto green ceramic tapes for electronic applications. *Mater. Sci. Eng.*, **177**: 1053-1066.
- Gao, M., Li, L. & Song, Y. (2017). Inkjet printing wearable electronic devices. *J. Mater. Chem. C*, **5**: 2971-2993.
- Huang, L., Huang, Y., Liang, J., Wan, X. & Chen, Y. (2011). Graphene-based conducting inks for direct inkjet printing of flexible conductive patterns and their applications in electric circuits and chemical sensors. *Nano Resear.*, **4**:675-684.
- Huang, X., Leng, T., Zhang, X., Chen, J.C., Chang, K. H., Geim, A.K. & Hu, Z. (2015). Binder-free highly conductive graphene laminate for low cost printed radio frequency applications. *Appl. Phys. Lett.*, **106**: 203105.
- Ismail, N., Salim, M. A., Naroh, A., Saad, A.M., Masripan, N.A., Donik, C. & Dai, F. (2020). The behaviour of graphene nanoplatelets thin film for high cyclic fatigue. *Int. J. Nanoelectr. Mater.*, **13**: 305-326.
- Kucinskis, G., Bajars, G. & Kleperis, J. (2013). Graphene in lithium ion battery cathode materials: A review. *J. Power. Sources*, **240**: 66-79.
- Lau, P.H., Takei, K., Wang, C., Ju, Y., Kim, J., Yu, Z. & Javey, A. (2013). Fully printed, high performance carbon nanotube thin-film transistors on flexible substrates. *Nano Lett.*, **13**: 3864-3869.
- Lee, Y., Choi, J.R., Lee, K.J., Stott, N.E. & Kim, D. (2008). Large-scale synthesis of copper nanoparticles by chemically controlled reduction for applications of inkjet-printed electronics. *Nanotech*, **19**: 415604.
- Leng, T., Huang, X., Chang, K., Chen, J., Abdalla, M.A. & Hu, Z. (2016). Graphene nanoflakes printed flexible meandered-line dipole antenna on paper substrate for low-cost RFID and sensing applications. *IEEE Antenn. Wirel. Propag. Lett.*, **15**: 1565-1568.

- Lu, K. (2012). *Nanoparticulate Materials: Synthesis, Characterization, and Processing*. John Wiley & Sons, Hoboken, New Jersey.
- Mokhlis, M., Salim, M.A., Masripan, N.A., Saad, A.M., Sudin, M.N., Omar, G. & Caridi, F. (2020). Nanoindentation of graphene reinforced epoxy resin as a conductive ink for microelectronic packaging application. *Int. J. Nanoelectr. Mater.*, **13**: 407-418.
- Nash, C., Spiesschaert, Y., Amarandei, G., Stoeva, Z., Tomov, R.I., Tonchev, D. & Glowacki, B.A. (2015). A comparative study on the conductive properties of coated and printed silver layers on a paper substrate. *J. Electron. Mater.*, **44**: 497-510.
- Nie, X., Wang, H. & Zou, J. (2012). Inkjet printing of silver citrate conductive ink on PET substrate. *Appl. Surf. Sci.*, **261**: 554-560.
- Oliver, W.C. & Pharr, G.M. (2004). Measurement of hardness and elastic modulus by instrumented indentation: Advances in understanding and refinements to methodology. *J. Meter. Res.*, **19**: 3-20.
- Rosa, P., Câmara, A. & Gouveia, C. (2015). The potential of printed electronics and personal fabrication in driving the internet of things. *Open J. Internet Things*, **1**: 16-36.
- Saad, H., Salim, M.A., Masripan, N.A., Saad, A.M. & Dai, F. (2020). Nanoscale graphene nanoparticles conductive ink mechanical performance based on nanoindentation analysis. *Int. J. Nanoelectr. Mater.*, **13**: 439-448.
- Singh, E., Meyyappan, M. & Nalwa, H.S. (2017). Flexible graphene-based wearable gas and chemical sensors. *ACS. Appl. Mater. Inter.*, **9**: 34544-34586.
- Suherman, H., Sahari, J. & Sulong, A. B. (2013). Effect of small-sized conductive filler on the properties of an epoxy composite for a bipolar plate in a PEMFC. *Ceram. Int.*, **39**: 7159-7166.
- Tang, L. C., Wan, Y. J., Yan, D., Pei, Y. B., Zhao, L., Li, Y.B. & Lai, G.Q. (2013). The effect of graphene dispersion on the mechanical properties of graphene/epoxy composites. *Carbon*, **60**: 16-27.
- Tortorich, R.P., Shamkhalichenar, H. & Choi, J.W. (2018). Inkjet-printed and paper-based electrochemical sensors. *Appl. Sci.*, **8**: 288.
- Van Den Brand, J., de Kok, M., Koetse, M., Cauwe, M., Verplancke, R., Bossuyt, F. & Vanfleteren, J. (2015). Flexible and stretchable electronics for wearable health devices. *Solid-State Electr.*, **113**: 116-120.
- Vasiljevic, D.Z., Menicanin, A.B. & Zivanov, L. D. (2013, April). Mechanical characterization of ink-jet printed ag samples on different substrates. *Doctoral Conf. Comput. Electr. Ind. Syst.*. Springer, Heidelberg, Germany, pp. 133-141.
- Wajid, A.S., Ahmed, H.T., Das, S., Irin, F., Jankowski, A.F. & Green, M.J. (2013). High-performance pristine graphene/epoxy composites with enhanced mechanical and electrical properties. *Mactomol Mater. Eng.*, **298**: 339-347.
- Wei, J., Vo, T. & Inam, F. (2015). Epoxy/graphene nanocomposites—processing and properties: a review. *RSC Adv.*, **5**: 73510-73524.
- Wu, W. (2017). Inorganic nanomaterials for printed electronics: a review. *Nanoscale*, **9**: 7342-7372.